

Dynamic modal analysis and synthesis of RSCR spatial mechanism

Muhsin J.Jweeg,^{*} Fahim Al-Himdani,^{**}
Mazin Ismail^{***}

Received on : 3/10/2004

Accepted on : 7/9/2005

Abstract

In this work ,analysis and synthesis of RSCR (Revolute –Spherical-Cylindrical –Revolute) spatial mechanism is presented. This work is based on the Hartenberg-Denavit 4 x 4 matrix method for the geometric characteristics of the mechanism involving the following three cases : the cylindrical ,the conical and the one-sheet hyperboloid .These cases derive their names from the nature of the locus of the slider of the linkage as viewed from the output side .Each case is then treated separately by analyzing displacement , velocity ,acceleration ,dynamic force and dynamic torque in each joint.

Also, method based on a Lagrangian formulation is presented to modelize the RSCR mechanism. A finite element model is used to study the structural behavior of the links, using the displacements referenced in the rigid body motion configuration as degrees of freedom . The finite element model is combined with the 4 x 4 matrix dynamics formulation and the equations of motion are derived from the lagrangian of the system . Existing VisualNastran 2002 -type finite element structural analysis program are combined with 4 x 4 matrix dynamic analysis techniques to yield a procedure capable of computing Free (Modal) Vibration for each case .

Several numerical examples are included in this work, and it was found that the best situation of the mechanism to be in a certain input angle range for cylindrical case. While for one-sheet hyperboloid, the mechanism works in a limited input angle range similar to the cone case, and as a result , the mechanism is considered as a rocker -- rocker type .

Keywords: Spatial mechanism , Mode shapes ,Finite element

الخلاصة

في هذا الفصل تمت دراسة الآلية RSCR الفضائية حيث ان المختصرات هذه ترمز الى نوعية المفاصل المستخدمة (R- دوراني ، S- كروي ، C- اسطواني ، R- دوراني) . هذا العمل مبني على التحليل بطريقة مصفوفة هارتنبيرغ - دينافيت (وهي مصفوفة ذات 4 × 4 عناصر) لثلاث هينات تركيبية لالوية : الاسطوانية ، المخروطية والقطع الزائد المجسم ، هذه الحالات اتخذت اسمائها من طبيعة الموقع الهندسي للمفصل الاسطواني عندما ينظر للشكل من منظور خارجي . كل حالة تمت معاملتها على انفراد حيث تم تحليل : الازاحة ، السرعة ، التعجيل ، القوى الحركية ، والعزوم الحركية عند كل مفصل .

كذلك تم تمثيل الآلية RSCR بالاعتماد على طريقة تمثيل لاكرانج ، ولغرض دراسة السلوك الهيكلي للاضلع تم استخدام نموذج عناصر محددة ، باستخدام طريقة مصدر الازاحات مع حركة

* Mech. Eng. Dept. Al-Nahrain University

**Mech. Eng. Dept. Al-Mustansiria Univ.

***Eng. mazinismail71@yahoo.com

الجسم غير المرن ، كذلك تم دمج نموذج العناصر المحددة مع مصفوفة الحركة (4×4) وبذلك تم الحصول على معادلة الحركة عن طريق معادلة لاكرانج للنظام ، ثم استخدام برنامج الحركة بواسطة مصفوفة (4×4) وبالنتيجة حساب الاهتزاز الحر (الترنسكيب) لكل حالة .
اشتمل البحث على امثلة حسابية ، حيث وجد ان افضل وضع للالية في مجال محدد بالنسبة الى المفصل الدوراني الخارجي للحالة الاسطوانية حيث انه (مرفقي - مرفقي) بينما لحالة القطع الزائد المجسم يعمل ضمن مجال مشابه لحالة المخروطي لذلك فهما اليقان من النوع (متآرجح - متآرجح) .

Nomenclature

A_o	= position of the input crank center
B	= position of the spheric pair
C	= position of the cylindric pair
F_o	= position of the output crank center
U_a	= unit vector representing the orientation of the input revolute axis
m	= axial distance of the slider from a reference point
h_h	= length of the coupler
S_j	= Transformation Matrix to define a coordinate system
α	= angle between cylindrical pair axis and coupler in their plane
ϕ	= rotation of the input crank
ψ	= angular position of the output crank
$\alpha_x, \alpha_y, \alpha_z$	= components of the angular acceleration

Introduction

In 1978 ,Hunt,K.H.^[1] studied the geometrical conditions of a stationary configuration for the linkage of (Revolute-Spherical-Cylindrical-Revolute). Osman, M.O.M.^[2] analyzed the spatial mechanism using " Train Component " and presenting iterative methods of analysis for a cylindrical case with limited angle only. Furthermore, Davidson , J.K.^[3] studied the case of one sheet hyperboloid for the Robot workspace. The main analysis in this paper has been applied using the analysis and optimal synthesis of the RSCR mechanism which was used by Ananthasuresh, G. K.^[4] inspite of analyzing the three cases (cylinder, cone and one sheet hyperboloid) the method is limited to the displacement only, and it used the geometry-based analysis .

There are a different methods which are used in analyzing the mechanisms like Yuan, M.S.C. and Freudenstein ,F.^[5] presents screw coordinates method . Kang ,H.Y. and Suh,C.H.^[6] developed Synthesis and Analysis of spherical -cylindrical (SC) link by a vector method., while , Zou,H.L and at el.^[7] studies the effect of variation in mechanism design using concepts of virtual displacement and rotation .A recursive formulation is introduced to obtain the state variation of a body in terms of the state variation of a junction body and of the relative coordinates along the chain. However, all thus above studies mentioned are for limited angle, and also it is very difficult for programming by the computer.

Sandor, G. N. and Erdman, A.G.^[8] also Shigley,J.E. and Uicker, J. R.^[9] used Denavit-Hartenberg 4×4

Matrix Method to synthesis and analysis the spatial mechanism to find out the displacement, velocity and acceleration. Uicker, J. R.^[10] developed procedures for the dynamic force analysis of spatial linkage. Song, P.^[11] used the decomposition technique (i.e cutting the joints and changes the mechanism to an open loop) to simplify the mathematical solution.

In designing a high -performance mechanism for proper dynamic characteristics, The key factor is its natural frequencies, This is because of the settling times of its vibrations .Natural frequencies of a spatial mechanism system is influenced by the inertia and flexibility of the links and joints ,link orientation and components comprising the drive and load shafts. Link orientation (offsets) increase the flexibility of the mechanism system ,lowers its natural frequency. Finite element studies dealt primarily with the effect of mass and flexibility of the links and joints of mechanisms are

Sunada, W. and Dubowsky, S.^[12,13] introduced the application of F.E.M. to the dynamic analysis of flexible spatial & co-planer linkage systems ,also they studied the dynamic analysis and behavior of Industrial Robotic Manipulator with elastic members. Turcic, D.A. and Midha^[14] developed generalized equations of motion for the dynamic analysis of elastic mechanism system with practical application.

WEE Ë N, F.V.^[15] made a F.E. approach to three-dimensional Kinetoelastodynamics . Bricout, J.N. et al.^[16] ,developed a F.E.Model for the dynamics of flexible manipulators while Smaili, A. and Bagci, J.^[17] conducted experimental and F.E. modal analysis of planar mechanisms with three-dimensional geometries. Roy, J. et al.^[18] , presented structural design optimization and comparative analysis a new high performance robot arm via F.E.A. Finally

Gerstmayr, J. and Schoberl J.^[19] developed a three-dim. F. E. approach to flexible multibody system.

The RSSR mechanism can be used only for function generation due to a passive degree of freedom of its coupler , while RSCR mechanism can be used for the purposes of function , path and motion generation .

Spatial Kinematic Analysis

Fig.(1,2) shows the RSCR mechanism, points Ao & Fo are fixed while B and C are moving points. The locus of B is a circle in space in a plane that is normal to Uao with center at Ao. On other hand ,the locus of C ,as viewed from the output side, is a surface whose shape depends upon the relative orientation of the output crank axis and the cylindrical pair axis in that position. Three different cases can then be identified as shown in Fig.(1,a-b-c) .

In all the three cases , the coordinates of the spherical pair location (i.e, point B) is found in the first step [4]. Since this step is common to all cases it is discussed separately here. For any given value of the input crank rotation ϕ ,coordinates of point B can easily be calculated using the

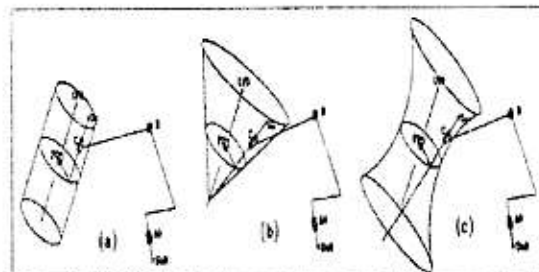


Fig (1) The three configurations of the RSCR mechanism

Uf_0 and U_c axes:	Locus of C
(a) parallel	Cylindrical surface
(b) Intersecting	Conical surface
(c) Skewed	One-sheet hyperboloid

Table No. (1) denavit – Hartenberg Notation .

- 1- $\alpha_{01} = 0$ $a = 0$ $\delta = h$ $\theta = \theta_1$
- 2- $\alpha_{12} = 90$ $a_{12} = p$ $\delta_{33} = 0$ $\theta = \theta_2$
- 3- $\alpha_{23} = 90$ $a_{23} = 0$ $\delta_{44} = 0$ $\theta = \theta_3$
- 4- $\alpha_{34} = 90$ $a_{34} = 0$ $\delta_{55} = 0$ $\theta = \theta_4$
- 5-a Conical : Rotation about y by $-\delta$
- b One sheet : Rotation about x by $-\delta$
- 6- $\alpha_{45} = 0$ $a_{45} = h$ $\delta = 0$ $\theta = \theta_5$
- 7- $\alpha = 0$ $a = 0$ $\delta = -m$ $\theta = 0$
- 8- $\alpha = 0$ $a = -r$ $\delta = 0$ $\theta = 0$
- 9- $\alpha = 0$ $a = 0$ $\delta = 0$ $\theta = -\psi$

spatial rotation matrix described below.

$$[R,U] = \begin{bmatrix} u_x v \theta c \theta & u_x v \theta - u_s \theta & u_x v \theta - u_s \theta & 0 \\ u_x v \theta - u_s \theta & u_x v \theta c \theta & u_x v \theta - u_s \theta & 0 \\ u_x v \theta - u_s \theta & u_x v \theta - u_s \theta & u_x v \theta c \theta & 0 \\ 0 & 0 & 0 & 1 \end{bmatrix}$$

And u_x, u_y, u_z are the x, y and z components of U_{a0} , and $s \Phi = \sin \Phi$, $c \Phi = \cos \Phi$ and $v \Phi = \text{vers } \Phi = 1 - \cos \Phi$... For the remainder parts of the mechanism, as in fig (2), a general 4x 4 transformation matrices are used as follows:

$$\therefore S_{03} S_{34} S_{45} S_{56} S_{60} = I \dots (3)$$

General equation of the closed loop mechanism

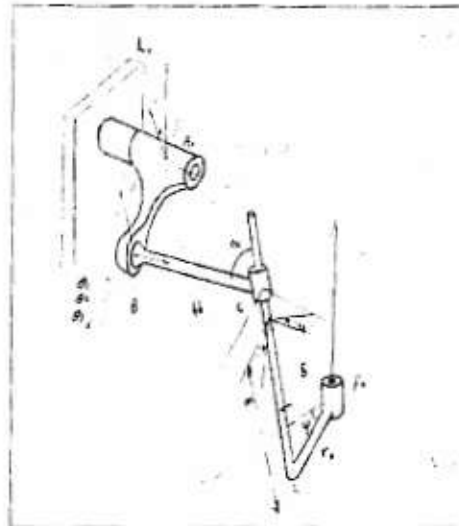


Fig (2) RSCR Mechanism

This equation states that ;as the loop is traversed ,and the dimensions of each link and the rotations and translations of each joint are considered , the coordinate system at the end is congruent with the one at the beginning .that is ,the product of all the matrices is equal to the identity matrix .this equation is called the loop-closure equation .It is a *nonlinear matrix* equation that must be solved during the position analysis of a mechanism.

Position analysis procedure

A general position analysis procedure is based on a Newton-Raphson iterative procedure [8] commonly used for the solution of nonlinear. For this procedure ,the “*Jacobian matrix*” for the non-linear equations is required . This is a matrix of the first partial derivatives of the equations with respect to the dependent variables of the mechanism.

A general loop-closure equation is written as:

$$S_{00} = S_{01}S_{12} \dots$$

$$S_{(k-1)k}(q_m)S_{k(k+1)} \dots S_{(n-1)n}S_{no}$$

Any one variable in a mechanism described by a loop-closure equation is wholly contained in only one of matrices making up the product. In the example shown, the variable denoted by q_m is contained in matrix $S_{(k-1)k}$ only.

$$\frac{\partial S_{00}}{\partial q_m} = S_{01}S_{12} \dots \frac{\partial S_{(k-1)k}(q_m)}{\partial q_m} S_{k(k+1)} \dots S_{(n-1)n}S_{no}$$

where Q_i the proper type of derivative operator matrix for the $S_{(k-1)k}$ matrix.

Let

$$I = (S_{01}S_{12} \dots S_{(k-1)k})^{-1} (S_{01}S_{12} \dots S_{(k-1)k}) \dots \dots \dots (6)$$

$$\frac{\partial S_{00}}{\partial q_m}$$

$$= S_{01}S_{12} \dots S_{(k-1)k} Q_i S_{k(k+1)} \dots S_{(n-1)n}S_{no} \dots \dots \dots (7)$$

Consequently ;

$$\frac{\partial S_{00}}{\partial q_m}$$

$$= D_m S_{00}$$

$$\therefore D_m = (S_{01}S_{12} \dots S_{(k-1)k})^{-1} Q_i (S_{01}S_{12} \dots S_{(k-1)k})$$

Where D_m : the derivative operator matrix with respect to the m -th variable in the loop.

A general 4×4 matrix made up of a product of 4×4 elementary transformation on matrices:

$$S_{0k} = \begin{bmatrix} r_{11} & r_{12} & r_{13} & \Delta_x \\ r_{21} & r_{22} & r_{23} & \Delta_y \\ r_{31} & r_{32} & r_{33} & \Delta_z \\ 0 & 0 & 0 & 1 \end{bmatrix} \dots \dots \dots (8)$$

The derivative operators for the rotational matrices are :

$$D_m^i = S_{0k} Q_i S_{0k}^{-1} =$$

$$\begin{bmatrix} 0 & -r_{31} & r_{21} & \Delta_y r_{31} - \Delta_x r_{21} \\ r_{31} & 0 & -r_{11} & \Delta_x r_{31} - \Delta_y r_{11} \\ -r_{21} & r_{11} & 0 & \Delta_x r_{21} - \Delta_y r_{11} \\ 0 & 0 & 0 & 0 \end{bmatrix}$$

$$i=1,2,3$$

For the translation-only matrix are :

$$D_m^i = S_{0k} Q_i S_{0k}^{-1} =$$

$$\begin{bmatrix} 0 & 0 & 0 & r_{1(i-3)} \\ 0 & 0 & 0 & r_{2(i-3)} \\ 0 & 0 & 0 & r_{3(i-3)} \\ 0 & 0 & 0 & 1 \end{bmatrix}$$

$$i=4,5,6$$

Position Analysis (Newton-Raphson):

$$S_{00} = S_{01}S_{12}S_{23} \dots \dots \dots (9)$$

$$S_{(n-1)n}S_{no} = I \dots \dots \dots (9)$$

Let $[q_I]$ = the vector of independent (joint) motion variables.

Let $[q_D]$ = the vector of dependent (joint) motion variables.

Expressed in terms of the variables as defined above , the non-linear eq.

$$S_{00}(q_D, q_I) - I = 0 \dots \dots \dots (10)$$

Using (N-R) iteration procedure[8]. or:

$$S_{00}(q_D, q_I) - I + \sum_{i=1}^m \frac{\partial S_{00}(q_D, q_I)}{\partial q_i} \Delta q_i = 0$$

where m is the total number of all independent and dependent variables

$$\text{Or } S_{00} + \sum_{i=1}^m (DiS_{00} \Delta q_i) - I = 0 \dots \dots \dots (12)$$

$$\text{Or } \sum_{i=1}^m (Di \Delta q_i) = S_{00}^{-1} - I = [E(i,j)] \dots \dots \dots (13)$$

The matrix above is dependent on the geometry of the mechanism , and contains the required information of

configuration and dimension, in other word :

$$\begin{bmatrix} S_D & S_u & S_l \\ A & B & \\ (6-r) \times r & (6-r) \times (m-r) & \end{bmatrix} \begin{bmatrix} \Delta \bar{q}_D \\ \Delta \bar{q}_u \\ \Delta \bar{q}_l \end{bmatrix} = \begin{bmatrix} \bar{R}_1 \\ \bar{R}_2 \end{bmatrix}$$

These changes in the dependent variables are added to the current estimate :

$$\bar{q}_D \leftarrow \bar{q}_D + \{\Delta \bar{q}_D\}$$

This iteration procedure continues until the changes $\{\Delta q_D\}$ are small and S_{00} approaches the identity matrix.

Velocity analysis:

$$\frac{ds_{00}}{dt} = \sum_{i=1}^m \frac{\partial S_{00}}{\partial q_i} \frac{dq_i}{dt} = 0 \quad \dots(15)$$

$$\text{or } \sum_{i=1}^m D_i S_{00} \dot{q}_i = \sum_{i=1}^m D_i \dot{q}_i = 0 \dots(16)$$

Solving

$$\{ \dot{q}_D \} = -[S_D]^{-1} (\{ [S_u] \{ \dot{q}_u \} + [S_l] \{ \dot{q}_l \} \}) \dots(17)$$

Acceleration Analysis :

$$\sum_{i=1}^m \frac{\partial^2 S_{00}}{\partial q_i^2} \ddot{q}_i + \sum_{i=1}^m \sum_{j=1}^m \frac{\partial^2 S_{00}}{\partial q_i \partial q_j} \dot{q}_i \dot{q}_j = 0 \dots(18)$$

$$\therefore S_{00} = 1$$

$$\therefore \sum_{i=1}^m \frac{\partial S_{00}}{\partial q_i} \ddot{q}_i = \sum_{i=0}^m D_i \ddot{q}_i \dots(19)$$

$$\therefore \frac{\partial^2 S_{00}}{\partial q_i \partial q_j} =$$

$$\begin{matrix} S_{01} S_{12} \dots S_{(k-1)k} Q_k S_{k(k-1)} \dots S_{(l-1)l} \\ (q_i) Q_i S_{i(i+1)} \dots S_{(n-1)n} \end{matrix} \dots(20)$$

$$\text{or } \frac{\partial^2 S_{00}}{\partial q_i \partial q_j} = D_i D_j S_{00}$$

and

$$\begin{aligned} \therefore [G_m] &= \sum_{i=1}^m \sum_{j=1}^m \frac{\partial^2 S_{00}}{\partial q_i \partial q_j} \dot{q}_i \dot{q}_j \\ &= \sum_{i=1}^m \sum_{j=1}^m \bar{D}_i \bar{D}_j \dot{q}_i \dot{q}_j \end{aligned}$$

$$\therefore \sum_{i=1}^m D_i \ddot{q}_i + [G_m] = 0 \dots(21)$$

$$[S] \{ \ddot{q} \} = - \{ \bar{G} \}$$

$$\begin{bmatrix} S_D & S_u & S_l \\ A & B & \end{bmatrix} \begin{bmatrix} \ddot{q}_D \\ \ddot{q}_u \\ \ddot{q}_l \end{bmatrix} = \begin{bmatrix} -\bar{G}_{m1} \\ -\bar{G}_{m2} \end{bmatrix}$$

Solving:

$$\begin{aligned} \ddot{q}_D &= -[S_D]^{-1} (\bar{G}_{m1} + [S_u] \ddot{q}_u \\ &+ [S_l] \ddot{q}_l) \end{aligned}$$

Dynamic Force & Torque Analysis of RSCR Spatial Mechanism

The absolute velocity of a point on link l with coordinates $X_i Y_i Z_i$ is found by differentiating equation :

$$R_i = T_i r_i \quad i=2,3,\dots,7 \quad (\text{No. of variables} = 7 \text{ in the RSCR mechanism}) \quad (23)$$

Where ; R_i : the global coordinate system , r_i :the local coordinate system.

$$\text{and } T_i = S_1 S_2 \dots S_{i-1} \\ R_i = [1 \quad X_i \quad Y_i \quad Z_i]^T, \quad r_i = [1 \quad x_i \quad y_i \quad z_i]^T \dots(24)$$

$$\dot{R}_i = U_i r_i \dot{q}_1 \quad i=2,3,\dots,7 \dots(25)$$

where \dot{R}_i is the velocity of the point

$$\dot{R}_i = \frac{d}{dt} R_i = [\dot{X}_i \quad \dot{Y}_i \quad \dot{Z}_i]^T \quad i=2,3,\dots,7 \dots(26)$$

\dot{q}_i is the input velocity , U_i is the "velocity matrix" defined as [10]:

$$U_i = \sum_{j=1}^{i-1} B_j T_j q'_j \quad i=2,3,\dots,7 \quad \dots\dots\dots(27)$$

$$B_i = S_1 S_2 \dots\dots\dots S_{i-1} Q_i S_i \dots\dots S_7$$

$$i=1,2,\dots\dots,7$$

and q'_j is the derivative of pair variable q_j with respect to the input variable q_1 .

Consider a particle of mass dm on link i of the mechanism and having coordinates $X_i Y_i Z_i$ in the coordinate system of the link and $X_i Y_i Z_i$ in the frame (absolute) coordinate system . The kinetic energy of this particle is :

$$dH_i = \frac{1}{2} (\dot{X}_i^2 + \dot{Y}_i^2 + \dot{Z}_i^2) dm \quad \text{But by}$$

eq (26) this can be expressed as

$$dH_i = \frac{1}{2} Tr(\dot{R}_i \dot{R}_i') dm$$

$$\text{or } dH_i = \frac{1}{2} Tr(U_i r_i \dot{q}_i \dot{q}_i' r_i' U_i') dm \quad (29)$$

Integrating over the mass of the link

$$H_i = \frac{1}{2} Tr[U_i (\int r_i r_i' dm) U_i'] \dot{q}_i^2$$

$$J_i = \int r_i r_i' dm$$

$$i=2,3,\dots\dots\dots,7 \quad (30)$$

So the kinetic energy

$$H_i = \frac{1}{2} Tr(U_i J_i U_i') \dot{q}_i^2$$

$$i=2,3,\dots\dots\dots,6 \quad (31)$$

And for the entire linkage this summed over all moving links:

$$H = \frac{1}{2} \sum_{i=2}^7 Tr(U_i J_i U_i') \dot{q}_i^2 \quad (32)$$

Suppose for a moment that of these constraints were removed , that one of the dimensional parameters , say hh , were free to change . This change is a variation of the constraint , denoted as

Δ . The system now has two degrees of freedom, q_1 and Δ . Notice that when the constraint hh was held constant there was a stress produced in that link by the inertia of the other moving links. When the constraint is allowed to move freely, this stress is removed. Suppose that an external force P is applied in place of the missing constraint force Then this applied force P must be the same as the constraint force which was removed .In each joint of the linkage there are three forces and three moments which must be evaluated.

The valid loop equation with a deformation between link i and link $i+1$ is :

$$S_1 S_2 \dots\dots\dots S_{i-1} (I + Q \Delta \Delta)$$

$$S_i \dots S_7 = I \quad \dots\dots\dots(33)$$

where S_i is the transformation matrix and Q_Δ is an operator matrix consistent with particular deformation chosen.

and

$$B \Delta = S_1 S_2 \dots S_{i-1} Q \Delta S_i \dots S_7 \quad \dots (34)$$

The equation for the position of a point on link J will also be different . If link J comes before the deformation , i.e , if $j \leq i$, then

$$R_j = S_1 S_2 \dots\dots\dots S_{j-1} r_j \quad j=2,3,\dots\dots,i$$

$$\dots\dots\dots(35)$$

However , if link j comes after the deformation , the position of the point is given by

$$R_j = S_1 S_2 \dots S_{j-1} (I + Q \Delta \Delta) S_i \dots S_{j-1} r_j$$

$$j=i+1,\dots,7 \quad \dots(36)$$

The velocity of a point on one of the moving links is found by time differentiating eq (36) . The result is :

$$R_j = U_j r_j \dot{q}_1 + U_{j\Delta} r_j \dot{\Delta} \quad j=2,3,\dots,7$$

$$(37)$$

The two "velocity component matrices" are defined as:

$$U_{ji} = \sum_{a=1}^{j-1} s_1 s_2 \dots s_a - 1 Q_a s_a \dots s_{j-1} q_a$$

$$+ \sum_{a=1}^{j-1} s_1 s_2 \dots s_a - 1 Q_a s_a \dots s_{i-1} Q_{\Delta} s_i \dots s_{j-1} q_a \Delta u_{ji}$$
(38)

$$U_{j\Delta} = \sum_{a=1}^{j-1} s_1 s_2 \dots s_a - 1 Q_a s_a \dots s_{j-1} q_a \Delta$$

$$+ \sum_{a=1}^{j-1} s_1 s_2 \dots s_a - 1 Q_a s_a \dots s_{i-1} Q_{\Delta} s_i \dots s_{j-1} q_a \Delta u_{ji}$$

$$+ s_1 s_2 \dots s_{i-1} Q_{\Delta} s_i \dots s_{j-1} q_i$$
(39)

Sub in (32) to get :

$$H = \frac{1}{2} Tr \sum_{a=2}^7 U_{a1} J_a U_{a1}^t q_1^2$$

$$+ \frac{1}{2} Tr \sum_{a=2}^7 U_{a\Delta} J_a U_{a\Delta}^t \Delta^2$$

$$+ \frac{1}{2} Tr \sum_{a=2}^7 U_{a1} J_a U_{a\Delta}^t q_1 \Delta$$
(40)

Dynamic Joints Reactions

Consider now the Lagrange equation describing the motion of the varying constraint

$$\frac{d}{dt} \left[\frac{\partial H}{\partial \dot{\Delta}} \right] - \frac{\partial H}{\partial \Delta} = F_d = -P$$
(41)

F_d is the dynamic force applied in the moving constraint to overcome the inertia of the links. P is the unknown force, the bearing reaction in the direction of the varying constraint due to the inertia of the moving links.

To produce a positive variation Δ , work must be done by the system against the force P ; thus the negative sign.

When the expression for kinetic energy, eq (40), is substituted into eq (41), the differentiation performed and terms in $\dot{\Delta}$ and Δ set equal to zero [10]; So

$$P = -Tr \sum_{a=2}^7 U_{a1} J_a U_{a1}^t \dot{q}_1^2 - Tr \sum_{a=2}^7 \frac{\partial U_{a1}}{\partial \Delta} J_a U_{a1}^t \dot{q}_1^2$$

$$-Tr \sum_{a=2}^7 U_{a1} J_a \frac{\partial U_{a1}}{\partial q_1} \dot{q}_1^2 + \frac{1}{2} Tr \sum_{a=2}^7 \frac{\partial U_{a1}}{\partial \Delta} J_a U_{a1}^t \dot{q}_1^2$$

$$+ \frac{1}{2} Tr \sum_{a=2}^7 U_{a1} J_a \frac{\partial U_{a1}}{\partial \Delta} \dot{q}_1^2 \dots (42)$$

Noticing that the trace of a matrix is equal to the trace of its transpose, the last two terms combine to give

$$P = -Tr \sum_{a=2}^7 U_{a1} J_a U_{a1}^t \dot{q}_1^2 - Tr \sum_{a=2}^7 \frac{\partial U_{a1}}{\partial q_1} J_a U_{a1}^t \dot{q}_1^2$$

$$- Tr \sum_{a=2}^7 U_{a1} J_a \frac{\partial U_{a1}}{\partial q_1} \dot{q}_1^2 + Tr \sum_{a=2}^7 U_{a1} J_a \frac{\partial U_{a1}}{\partial \Delta} \dot{q}_1^2$$

The partial derivatives required in this expression can be found by differentiating equations (38) and (39) and evaluating the results at $\Delta = 0$. Thus

$$\frac{\partial U_{a1}}{\partial q_1} / \Delta = 0 = \sum_{b=1}^{a-1} \sum_{c=1}^{a-1} s_1 s_2 \dots s_b - 1 Q_b s_b \dots s_c - 1 Q_c s_c \dots s_a - 1 q_b q_c$$

$$+ \sum_{b=1}^{a-1} s_1 s_2 \dots s_b - 1 Q_b s_b \dots s_a - 1 q_b$$

$$= \sum_{b=1}^{a-1} B_b T_a q_b + \sum_{b=1}^{a-1} \sum_{c=1}^{a-1} B_b B_c T_a q_b q_c$$

where q_b'' is the second partial derivative of q_b with respect to the input variable q_1 , and $\overline{B_b B_c}$ is defined as :

$$\overline{B_b B_c} = s_1 s_2 \dots s_b - 1 Q_b s_b \dots s_c - 1 Q_c s_c \dots s_7$$

$$= \begin{cases} B_b B_c & \text{for } b \leq c \\ B_c B_b & \text{for } b > c \end{cases} \dots (45)$$

In a similar fashion

$$\frac{\partial U_{a\Delta}}{\partial \Delta} / \Delta = 0 = \sum_{b=1}^{a-1} \overline{B_b B_c} T_a q_b \Delta + \sum_{b=1}^{a-1} \sum_{c=1}^{a-1} \overline{B_b B_c} T_a q_b \Delta q_c$$

Where $\overline{B_b B_c}$ is defined in a fashion

similar to equation (45) and $q_{b,d}$ and $q_{b,d}''$ are defined as :

$$q_{b,d}' = \frac{\partial q_b}{\partial \Delta} \dots\dots(47)$$

$$q_{b,d}'' = \frac{\partial^2 q_b}{\partial \Delta \partial q_i} \dots\dots(48)$$

Finally,

$$\frac{\partial U_{a,i}}{\partial \Delta} \Big|_{\Delta=0} = \sum_{b=1}^{a-1} B_b T_{b,d}'' + \sum_{b=1}^{a-1} \overline{B_b B_d} T_{a,b} q_b' + \sum_{b=1}^{a-1} \sum_{c=1}^{a-1} \overline{B_b B_c} T_{a,b} q_{b,d} q_c' \dots\dots(49)$$

The dynamic bearing reactions P can now be found by substituting these partial derivatives into equation (43). Expanding $U_{a,i}$ and $U_{a,d}$ according to their definitions and evaluating at $\Delta = 0$ leaves which gives the bearing reaction in the direction of Δ due to the inertia of the moving links :

$$P = -\gamma r \sum_{a=2}^n \left[\sum_{b=1}^{a-1} B_b q_b \right] \left[T_{a,i} J_a T_a' \left[B_a U_{a,i} + \sum_{c=1}^{a-1} B_c q_{c,d} \right] \ddot{q}_i - \gamma r \sum_{a=2}^n \left[\sum_{b=1}^{a-1} \left(B_b q_b'' + \sum_{c=1}^{a-1} \overline{B_b B_c} q_b' q_c' \right) \right] \times \left[T_{a,i} J_a T_a' \left[B_a U_{a,i} + \sum_{c=1}^{a-1} B_c q_{c,d} \right] \right]^2 q_i^2 \dots\dots\dots F = -\gamma r \sum_{a=2}^n \left[\sum_{b=1}^{a-1} B_b q_b'' \right] \left[T_{a,i} J_a T_a' \left[\sum_{c=1}^{a-1} B_c q_c' \right] \right]^2 \ddot{q} - \gamma r \sum_{a=2}^n \left[\sum_{b=1}^{a-1} \left(B_b q_b'' + \sum_{c=1}^{a-1} \overline{B_b B_c} q_b' q_c' \right) \right] \times \left[T_{a,i} J_a T_a' \left[\sum_{c=1}^{a-1} B_c q_{c,d} \right] \right]^2 q_i^2$$

Finite element Formulation :

The System Dynamic equations are assembled from the link dynamic equation $M_i \ddot{a}_i + G_i \dot{a}_i + K_i a_i = f_i^o$ (52) In general, the relationship of the reduced coordinate vector of the ith

link "a_i" and the global coordinate vector "q" is given by the familiar linear transformation [16]

$$a_i = B_i(\theta_i) . q \dots\dots\dots (53)$$

where B_i the "compatibility matrix" for the ith link and is, in general, a time- varying function of the nominal joint angles θ_i . For structures, the B_i matrices are constant. The system dynamic equations can now be written in global coordinates by taking the time derivatives of a_i given by equ.(53) and substituting them into eq.(52) for each link. The resulting equations are then pre-multiplied by B_i^T and summed over all the links, thus eliminating the unknown joint interface forces and producing the following global equations of motion.

$$M \ddot{q} + G \dot{q} + Kq = Q \quad (54)$$

where

$$M = \sum_{i=1}^{NL} B_i^T M_i B_i$$

$$G = \sum_{i=1}^{NL} B_i^T G_i B_i + \sum_{i=1}^{NL} \sum_{j=1}^{NL} 2 B_i^T M_i B_j \dot{\theta}_j + G_j$$

$$K = \sum_{i=1}^{NL} B_i^T K_i B_i + \sum_{i=1}^{NL} \sum_{j=1}^{NL} B_i^T G_i B_j \dot{\theta}_j (\dot{\theta}_j \dot{\theta}_k + B_{ij} \ddot{\theta}_j)$$

$$Q = \sum_{i=1}^{NL} B_i^T f_i^o$$

$$B_{ij} = \frac{\partial B_i}{\partial \theta_j} \quad B_{ijk} = \frac{\partial^2 B_i}{\partial \theta_j \partial \theta_k}$$

NL =no. of links in the mechanism.

The transfer function of the system to any periodic input Q , is obtained by assuming :

$$Q = \tilde{Q} e^{i\omega t} \dots\dots\dots(55)$$

Assuming the response \tilde{q} will also be periodic yields :

$$\tilde{q} = (-\omega^2 M + i\omega G + K)^{-1} \tilde{Q} \quad (56)$$

Finally ,the natural frequencies ω and mode shapes q for the stationary mechanism are obtained with a Householder QR eigenvalue procedure

Numerical Examples:

The first numerical example involves the cylindrical configuration. The second example for the cone configuration, while the third example for the one sheet hyperboloid. The optimum design position and orientation for these examples as shown in the tables below respectively, the material that used is steel.

The Result and Discussion

Fig.(3) shows the variation of the spherical joint angles $(\theta_x, \theta_y, \theta_z)$ versus

the time; where θ_x a negative curve (max. -84°); θ_z a positive curve (max $+66^\circ$) and θ_y a positive starts at

(zero $^\circ$) and increases to the max. (35°) and then decreases to the zero .Fig. (4) shows the orientation of the cylindrical joint time; it indicates it starts at zero then increase to (-0.115 m) then decrease to zero. Fig.(6) show the orientation of the output revolute ($\theta_s = \theta_y$) is plotted versus

the time; it should be seen that it start from (zero $^\circ$) then increase to max. (80°) at (45° input angle) then decrease to zero and finally increases to reach the max.

Table-2 Cylindrical case

Joint name	X mm	Y mm	Z mm	Rx deg	Ry Deg	Rz deg
Revolute inp	35.9	-116	134	41.9	5.51	-164
Rigid joint 1	26.3	-49.7	60.2	-138	-5.51	-16.1
Spher. joint	-27.1	40.3	74.3	-80.8	-30.3	4.66
Cylin. joint	-41.8	-27.8	35.7	180	0	180
Rigid joint 2	-41.8	-27.8	-110	0	0	0
Revolute output	0	0	-110	90	-56.4	-180

Connected rod: length =79.9 mm dia.=5 mm output link: length =30.2 mm dia.=5 mm

Table -3 Conical case

Joint name	X mm	Y mm	Z mm	Rx deg	Ry deg	Rz deg
Revolute inp	100	25.2	-23	0	-53.2	90
Rigid joint 1	20.1	25.2	37	0	-53.2	90
Spher. joint	28.7	-25.3	46.9	-7.47	0.25	-81.4
Cylin. joint	79.4	1.79	40.7	-1.56	50.4	-88
Rigid joint 2	30.2	0.678	0	0	1.53	-75.1
Revolute out	0	0	0	0	0	0

Connected rod: length =57.8 mm dia.=5 mm output link: length =30.2 mm dia.=5 mm

Table -4 One sheet hyperboloid case

Joint name	X mm	Y mm	Z mm	Rx deg	Ry deg	Rz deg
Revolute inp	100	25.2	-23	0	-53.2	90
Rigid joint 1	20.1	25.2	37	0	-53.2	90
Spher. joint	28.7	-25.3	37	76.9	9.49	-178
Cylin. joint	30.2	58.2	27.7	130	0	180
Rigid joint 2	30.2	0.678	-20	0	1.53	-75.1
Revolute out	0	0	0	0	0	0

Connected rod: length =85.7 mm dia.=5 mm output link: length =30.2 mm
dia.=5 mm

(+80°) at (180° input angle).

Fig.(7) shows the angular velocities of the spherical joint ($\omega_x, \omega_y, \omega_z$)

versus the time; it is seen that the mechanism is approximately stable at velocity (250 deg/s) between (35°~225°) input angle. Fig. (8) represents the angular velocity of cylindrical joint (ω_z) versus the

time; the angular velocity of the cylindrical decreases rapidly from max. to min. after the (180° input angle) then increases from min. to max. due to the coupler (floating link). Fig.(9) shows the linear velocity of cylindrical joint V_z versus the time; Fig.(10) shows the angular velocity of the output revolute joint (ω_y) versus the time. From all the velocities figures ; it can be seen that the sequence of the increases and decreases in the joint linear or angular velocity components due to the positive or negative rate of change of the joint angles respectively .

Since $a=(V-V_0)/t$ and at ($t=0, V_0=0$) therefore the acceleration equal infinity at $t=0$. Fig.(11) shows the

angular acceleration. of the spherical joint ($\alpha_x, \alpha_y, \alpha_z$) versus the time. It

can be observed that the acceleration at the starting time is infinity. Fig.(12) shows the angular acceleration of the cylindrical joint (α_z) versus the time. Fig.(13) shows the linear acceleration. of the cylindrical joint (a_z) versus the time. Fig.(14) shows the angular acceleration (α_y) of the

output revolute versus the time. It can be seen that there is a sequence of the increases and decreases in the linear or angular acceleration due to the positive or negative rate of change of the angular or linear velocity respectively.

Because of $F=m.a$ and due to a equal infinity at the time = zero , so F equal infinity at that positions. Fig.(15~18) show the dynamic forces that arise on the connected bodies by the joints during the operation of the mechanism (F_x, F_y, F_z) versus the crank angle, it is clear that all the characteristics of the charts depends upon the acceleration values because of ($F=m.a$), it is clear that the best

operation input angle range is between $30^\circ \sim 330^\circ$ input angle. Because of (Torque $= I \cdot \alpha$) where I is the moment of inertia and due to α equal infinity at the starting zero so (T equal infinity) at these position. It is clear that there is no torques at the spherical joint due to their physical properties. Fig.(19~22) show the dynamic torques that arise on the connected bodies by the joint during the operation of the mechanism (T_x, T_y, T_z) versus the crank angle it is clear that all the characteristics of the charts depends upon the acceleration values because of ($T = I \cdot \alpha$).

Fig.(23~27) show the variations in the first, second, third, fourth, and fifth natural frequency with crank angle for (RSCR) cylindrical spatial mechanism case for complete rotation ($0 \sim 360^\circ$) using (10-node parabolic tetrahedron brick element) (# elements = 450, # nodes = 957). As expected, an inherent characteristic of such mechanism is verified in that they manifest very large variations in their natural (modal) frequency with position, so this illustrates the importance of including vibration effects in the analysis of high speed RSCR spatial mechanism. The natural frequency depends on the [K] stiffness matrix, since this matrix depends on the orientation of the mechanism which leads to a variant values of the natural frequency with the change of the crank (input) angle.

The point of maximum stress fall on the follower link.

Fig. (28-a,b,c,d,e) show the deformed shapes for the fifth modes of free vibration for the (RSCR) cylindrical case spatial mechanism at (40°) input angle

Conclusions

1- The output configuration in the cylindrical joint leads to give three cases: cylindrical, conical and hyperboloid therefore this mechanism can be used after fixing a cutting tool in the cylindrical joint, to produce three kinds of gears or painting or welding machine.

2- With respect to the input crank, the output revolute angle, and the follower traction – as indicated in the scenario of each case – it was found that:

a- Cylindrical case (360°) so: double crank mechanism.

b-Conical case (240°) so: rocker-rocker mechanism.

c-One-sheet hyperboloid (235°) so: rocker - rocker mechanism.

3-The best operation range of angle for :

a-Cylindrical case is between $35^\circ \sim 240^\circ$ input angle .

b-Conical case is between $0^\circ \sim 40^\circ$ and $70^\circ \sim 220^\circ$ input angle

c-One-sheet case is between $0^\circ \sim 180^\circ$ input angle .

Where all the forces tend to be a small amount & constant (i.e. a small input power to operate this mechanism) in contrast, all the other values

(displacement, velocity, acceleration) are constant approximately.

4- The large variations in the natural (modal) frequencies with respect to crank position, indicates the importance of including vibration effects in the analysis of high speed RSCR mechanism.

5-In designing a high-performance mechanism like (RSCR) mechanism for proper dynamic characteristics, the key factor is its natural frequencies, this is because of the settling times of its vibrations. Natural frequencies of a spatial mechanism system (i.e. RSCR) is influenced by the inertia and flexibility of the links and joint, link orientation and components comprising the drive and load shafts. Link orientation (offsets) increase the flexibility of the mechanism system, lower its natural frequency.

6-The follower link is the main member which received a great amount of the vibration forces. So, to ensure successful design for RSCR mechanism, length, cross-section and the material of the mechanism must be taken into the account.

References

1. Hunt, K. H. "Kinematic Geometry of Mechanisms" Clarendon Press-Oxford.
2. Osman, M.O.M., Bahgat, B.M. and Dukkupati, R.V., J. of Mech. Design, Vol.103, P.(823-830). Oct.(1981).
3. Davidson J.K., Hunt K. H., Transaction of The ASME, "Robot Workspace of a Tool Plane Part-1: A ruled Surface and Other Geometry. Part-2- Computer Generation and Selected Design Condition for Dexterity". vol.109, MARCH (1987).
4. Ananthasuresh, G.K., Kramer, S.N. Transaction of The ASME 174-181, "Analysis and Optimal Synthesis of The RSCR Spatial Mechanism", Vol.116, March-(1994).
5. Yuan M.S.C., Freudenstein F. J., of Eng. for Industry, "Kinematic Analysis of Spatial Mechanisms by Means of Screw Coordinates Part 1& 2", Feb.(1971).
6. Kang H.Y., Suh, C.H. "Synthesis and Analysis of Spherical - Cylindrical (SC) Link in The McPherson Strut Suspension Mechanism by of Mech. Design, vol.116 (599-606), June (1994).
7. Zou H.L., Abdel-Malek K., Wang J. Y., "A Variational Approach for The Design of The Spatial Four-Bar Mechanism", Mechanics of Structures of Machines, Vol.25, No.1, pp 41-59, (1997).
8. Sandor N. George, Erdman G. Arther "Advanced Mechanism Design: Analysis and Synthesis

- Volume-2", Prentice-Hall, Inc. New Jersey, (1984).
9. Shigley, J. E., Uicker J. J., Jr. "Theory of Machines and Mechanisms", 2nd ed., McGraw-Hill, (1995).
 10. Uicker, J. J. Jr., "Dynamic Force Analysis of Spatial Linkages" Transaction of The ASME June pp(418-424), (1967).
 11. Song P., "Modeling, Analysis and Simulation of Multibody Systems with Contact and Friction", a Dissertation, Pennsylvania University, USA. (2002).
 12. Sunada W., Dubowsky S., "The Application of Finite Element Methods to The Dynamic Analysis of Flexible Spatial and Co-planer Linkage Systems", J. of Mech. Design, July, Vol.103 pp(643-656), (1981).
 13. Sunada W., Dubowsky, S., "On The Dynamic Analysis and Behavior of Industrial Robotic Manipulator with Elastic Members" Transaction of The ASME March ,vol.105 42-51, (1983).
 14. Turcic, D. A., Midha, A., "Generalized Equations of Motion for The Dynamic Analysis of Elastic Mechanism Systems", J. of Dyn. Sys., Meas. and Cont., vol.106 pp(243-254). Dec.(1984).
 15. Wee ã n, F.Vander "A Finite Element approach to three-Dim. Kinetoelasodynamics", J. of Mech. Mach. Theory Vol.23, No.6, pp.(491-500), (1988).
 16. Bricout, J. N., Debus, J. C., Micheau,p. "A finite Element Model For the Dynamics of Flexible Manipulators", J. of Mech. Mach. Theory Vol.25 No. 1 pp.(119-128), (1990).
 17. Smaili, A., Bagci, I., "Experimental and Finite Element Modal Analysis of Planer Mechanisms with Three-Dimensional Geomerics", J. of Mech. Design, Vol.120 PP.(401-403), Sep.(1998).
 18. Roy, Jaydeep, Whitecomb, Louis, L. Johns Hopkins University, Proceeding of the IEEE International Conference on Robotics and Automations. "Structural Design Optimization and Comparative Analysis of a New High-Performance Robot Arm via Finite Element Analysis", (1997).
 19. Gerstmayr, Johannes, Sch ð berl ,Joachim "A 3D Finite Element approach to flexible multibody systems " Fifth World Congress on Computational Mechanics July 7-12, Vienna, Austria, Eds: H. A. Mary, F. G. Rammerstorfer, Eberhardsteiner J., (2002).

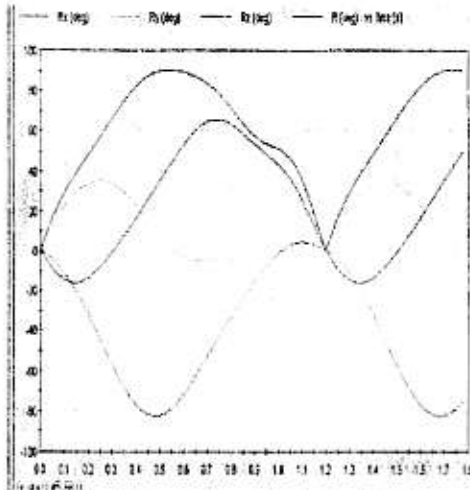


Fig. (3) rotation of spherical joint ($\theta_x, \theta_y, \theta_z, \theta$)

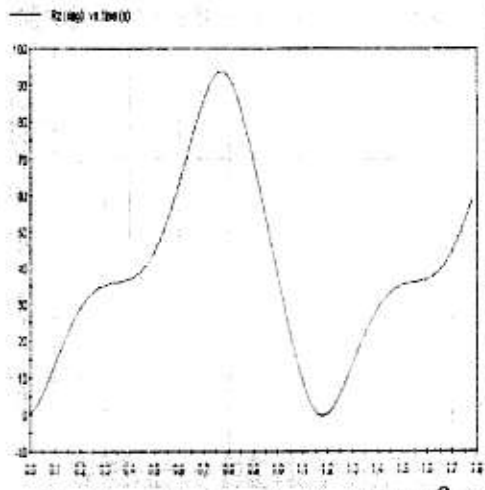


Fig. (4) rotation of cylindrical joint (θ_2)

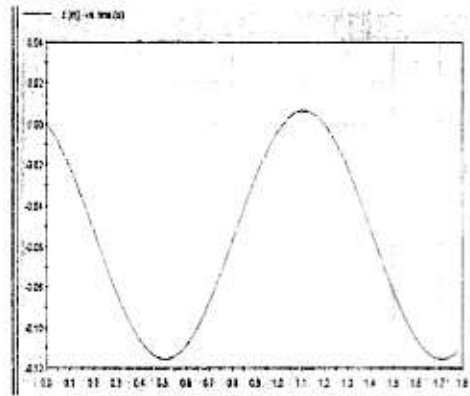


Fig. (5) Displacement of cylindrical joint (z)

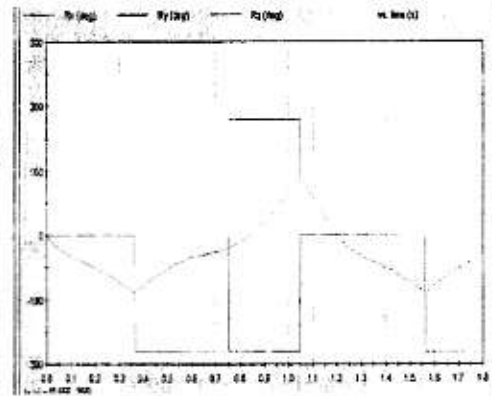


Fig. (6) rotation of output revolute joint (ψ)

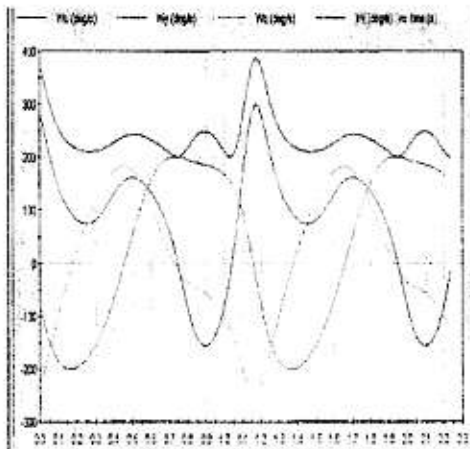


Fig. (7) Angular vel. of spherical joint ($\omega_x, \omega_y, \omega_z$)

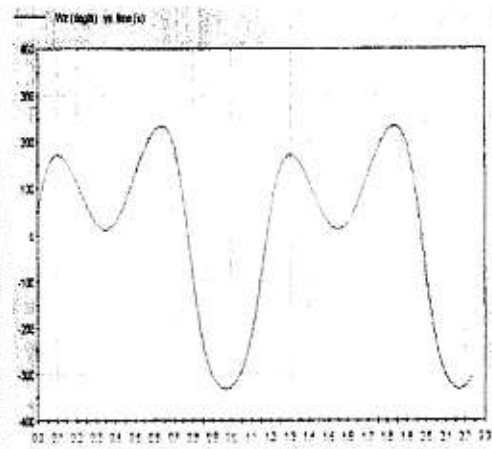


Fig. (8) Angular vel. of cylindrical joint (ω_2)

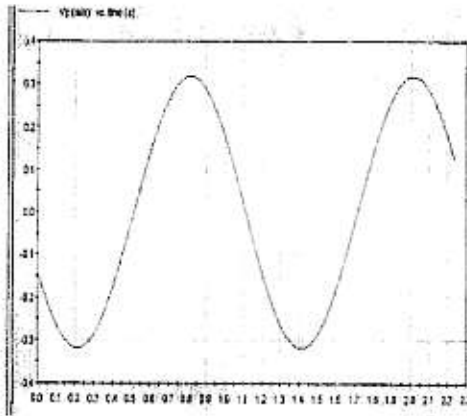


Fig. (9) Linear vel. of cylindrical joint (V_2)

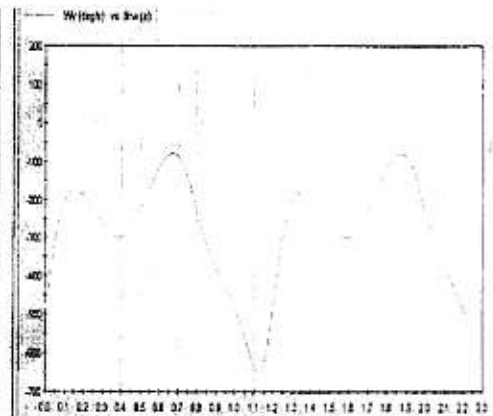


Fig. (10) Angular vel. of output revolute joint (ω_2)

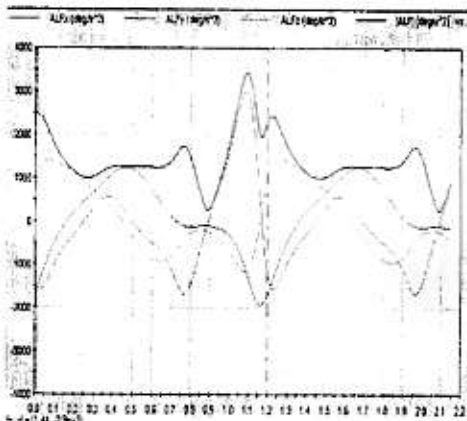


Fig. (11) Angular Accel. of Sph joint ($\alpha_x, \alpha_y, \alpha_z$)

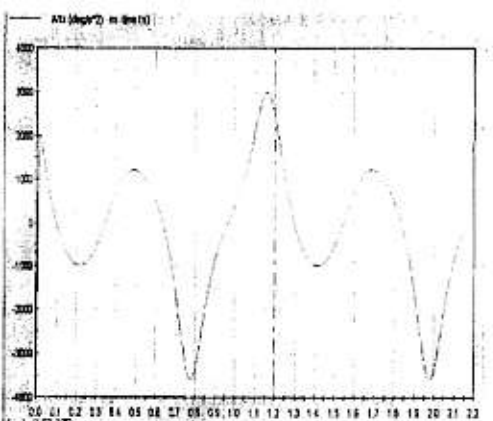


Fig. (13) Angular accel. of cylindrical joint (α_2)

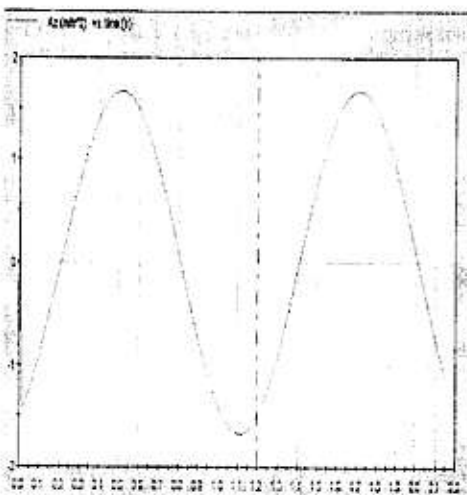


Fig. (13) Linear Accel. of cylindrical joint (a_2)

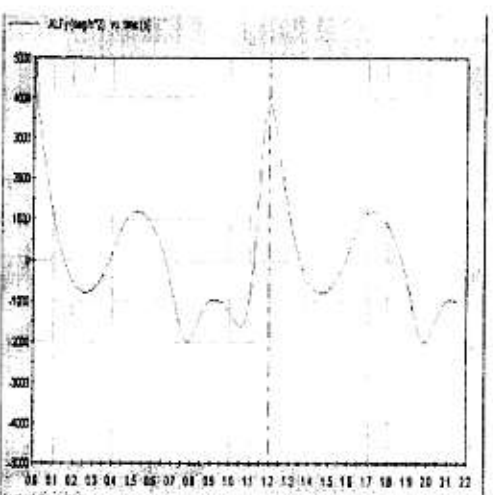


Fig. (14) Angular accel. of output revolute joint(α_2)

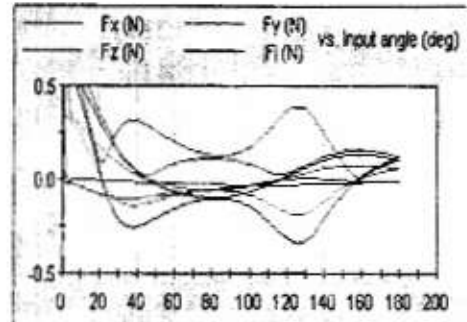
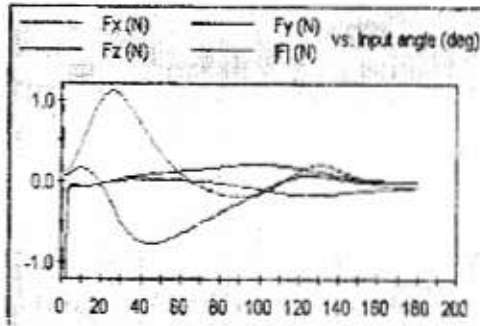


Fig.(16) Cylindrical joint Force on Output crank

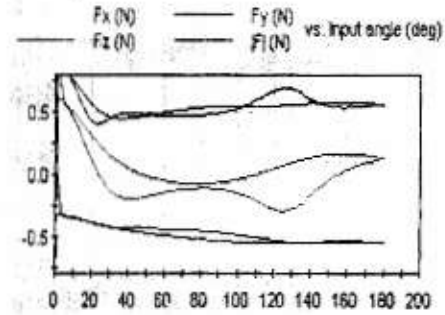
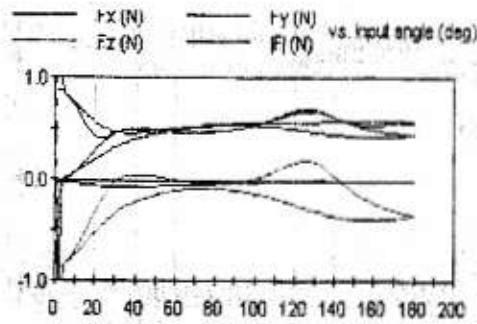


Fig.(18) Spherical joint Force on Coupler

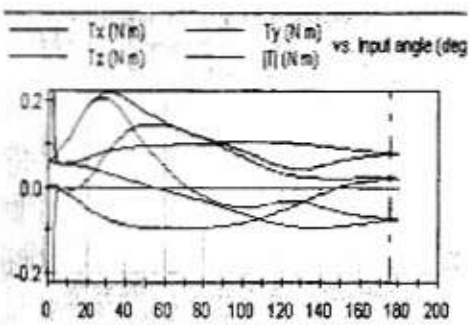
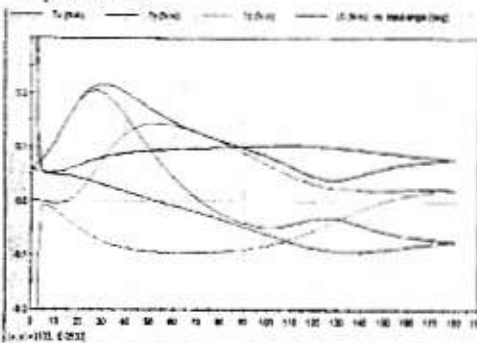


Fig.(19) Output Revolute Torque on output crank

Fig.(20) output crank Torque Output Revolute

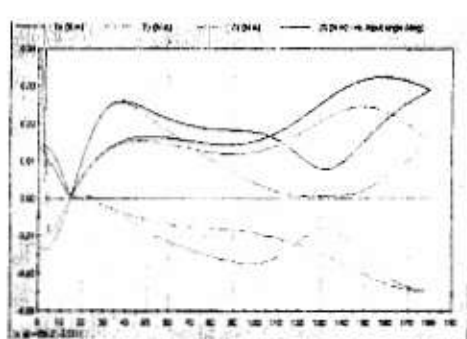
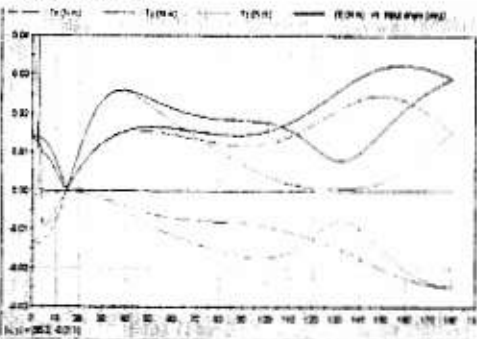


Fig.(21) Cylindrical joint Torque on the vertical crank

Fig.(22) the vertical crank Torque on Cylindrical joint

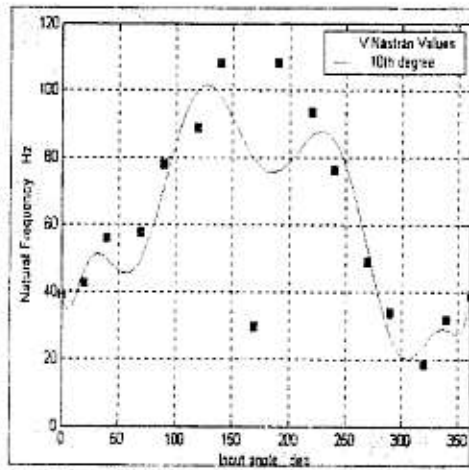


Fig. (23) First mode natural freq. versus crank angle

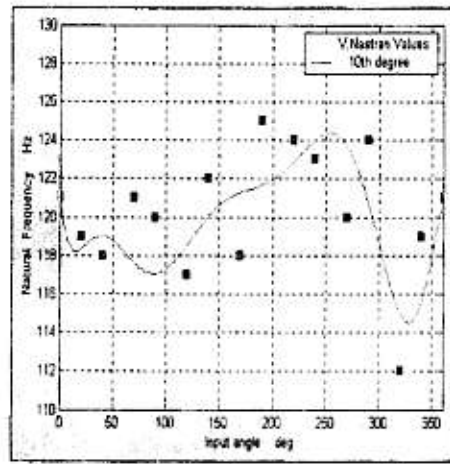


Fig. (24) Second mode natural freq. versus crank angle

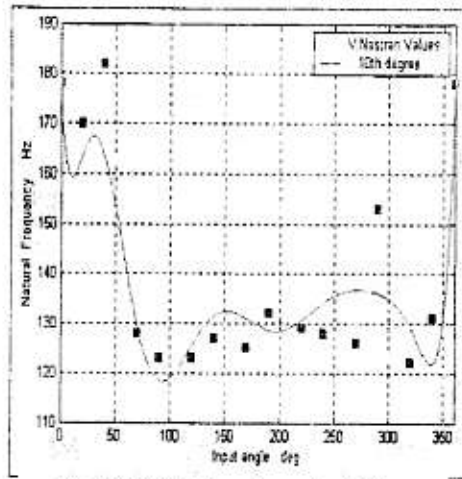


Fig. (25) Third mode natural freq. versus crank angle

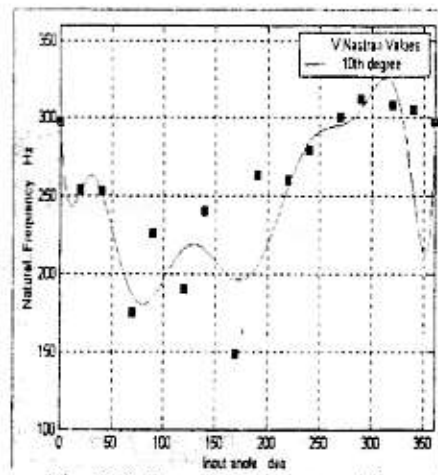


Fig. (26) Fourth mode natural freq. versus crank angle

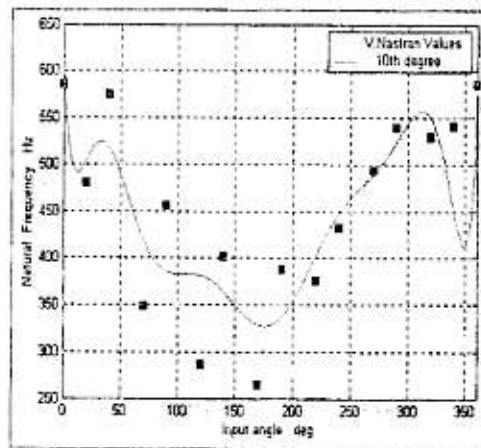


Fig. (27) Fifth mode natural freq. versus crank angle

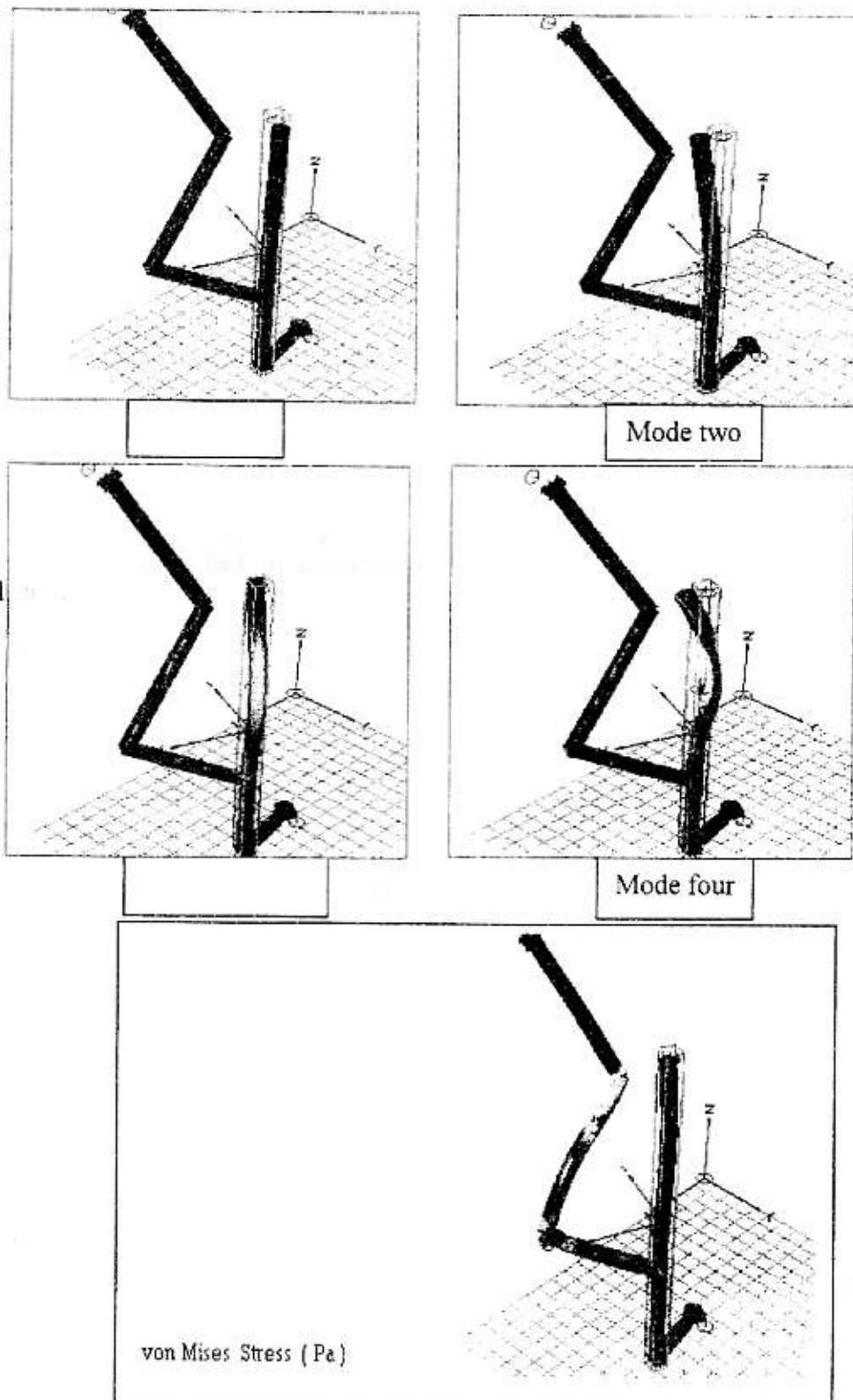


Fig (28) Five deformed shapes for RSCR mechanism Cylindrical case using finite element (V. Nastran 2002 program)